Critical behavior of a dynamic analog to the $q=3$ Potts model

Elena Salazar-Neumann, María Cristina Vargas,* and Gabriel Pérez
Departamento de Física Aplicada, Centro de Investigación y de Estudios Avanzados del Instituto Politécnico Nacional, Unidad Mérida Apartado Postal 73 "Cordemex," 97310 Mérida, Yucatán, Mexico
(Received 16 April 2004; published 31 March 2005)

We construct a dynamical analog to the $q=3$ Potts model, using linear chaotic maps and a diffusive coupling. We find well-defined order-disorder phase transitions (PTs) in the system, and obtain the phase diagrams for both simultaneous and sequential updating of the model. For simultaneous updating we find continuous PTs whose critical exponents are consistent with those of the equilibrium Potts model. Under sequential updating, the phase diagram shows a tricritical point, and the PTs become first order for large coupling and chaoticity of the local maps. A preliminary estimation finds critical exponents in the region of continuous PTs that are not consistent with those of the equilibrium model.

DOI: 10.1103/PhysRevE.71.036228 PACS number(s): 05.45.Ra, 64.60.−i

I. INTRODUCTION

Coupled map lattices (CMLs)—dynamical systems with discrete-time, discrete-space, and continuous states, consisting of interacting elements on a regular lattice—have been the subject of intense research during the last several years, mainly because they have proven to be suitable simple models of extended dynamical systems [1–7]. CMLs may be used to simulate complex phenomena in physics and other fields such as chemistry, biology, computation, engineering, and even social sciences [8]. Most of the interest in these systems has been concentrated in their possible collective behavior; in fact, it has been found that some types of chaotic CMLs present order-disorder transitions with the same phenomenology found in continuous phase transitions (PTs) in equilibrium statistical mechanics. In particular, Miller and Huse [9] studied two-dimensional (2D) lattices of odd-symmetric piecewise-linear chaotic maps with diffusive coupling and found an order-disorder transition that was tentatively located in the 2D Ising universality class. Extensive calculations for this and other similar models performed by Marcq *et al.* [10,11] indicate that the transition does not really belong to the 2D Ising universality, since the critical exponent for the correlation length (ν) appears to be different from the Ising value ($\nu=1$) when the numerical simulations are done in such a way that the individual lattice sites are updated synchronously. On the other hand, it was also found that asynchronous updating of the lattice sites brings the PT back to the 2D Ising universality, suggesting that the updating scheme is a relevant parameter in the vicinity of the PT.

It has been generally believed that equilibrium spin systems, such as the ones represented by the Ising model, cannot be simulated by synchronous algorithms [12]. In the Metropolis Monte Carlo algorithm [13], for instance (which is the simplest and best known numerical simulation for these equilibrium systems), one cannot update two neighboring—in general, interacting—spins simultaneously [14]. In dynamical systems, on the other hand, the issue of simultaneous updating had been explored for extended systems with local interactions [7,15,16] and also for globally coupled systems [17–19]. Chaté and Manneville [7] found in 1992 that synchronicity is essential for systems with local interactions for exhibiting nontrivial collective behavior, concluding that any analogy with the traditional systems of statistical mechanics studied by using asynchronous algorithms should be made with great care. For globally coupled (mean-field-like) systems, Kaneko [17] found in 1990 that "globally coupled chaos violates the law of large numbers but not the central limit theorem." More recently, in 1998, Abramson and Zanette [18] showed that the dynamical behavior of asynchronous globally coupled maps is completely different from that of the usual synchronous models and also found that asynchronous updating restores the law of large numbers. This finding was corroborated by Sinha [19], whose studies also showed that the normal statistical behavior is rapidly restored with a certain degree of asynchronicity. A recent study explored the issue of whether or not the updating scheme is a relevant parameter in the dynamical behavior of locally coupled extended systems, using a simultaneous version of the well-known Metropolis algorithm for the simulation of the 2D Ising model [15]. It was found that, after a small modification done to the algorithm in order to rule away some anomalous behavior of the system, simultaneous updating in the Metropolis algorithm preserves the universality class of the Ising model, and so, in this case at least, the issue of synchronicity in updating is irrelevant. It was noted, however, that the "small modification" (actually, a reduction in the acceptance ratio for both increasing- and decreasing-energy moves) could be a source of asynchrony in the updating scheme.

The question about what makes the Miller-Huse [9] and some other models [10,11,20] show a critical behavior different from the expected Ising-like one is still unanswered. In this paper we perform a study of the phase transitions in CMLs with the symmetries of the $q=3$ Potts model, focusing our attention on the effects of the synchronization, or absence of it, in the updating scheme. In Sec. II we describe the model; Sec. III studies the model under simultaneous updating, and includes a description of the finite-size scaling tech-

*Electronic address: cristina@mda.cinvestav.mx

niques used. Asynchronous updating is studied in Sec. IV, and our final conclusions appear in Sec. V.

II. A DYNAMICAL ANALOG OF THE $Q=3$ POTTS MODEL

The dynamical system we study is modeled by a 2D square lattice, whose elements obey an individual dynamics given by the nonlinear chaotic map $x_{i,j}(t+1)=F(x_{i,j}(t))$, to be followed by a diffusive interaction of strength ϵ. The combination of these two steps gives the mapping

$$x_{i,j}(t+1) = F(x_{i,j}(t)) + \frac{\epsilon}{d}\sum_{i',j'} \mathcal{D}(F(x_{i',j'}(t)),F(x_{i,j}(t))), \tag{2.1}$$

where the sum is over the d nearest neighbors (i',j') of the site (i,j), and $\mathcal{D}(x,y)$ stands for the shortest distance between x and y, to be defined later.

As for the local map, our goal is to generate one that is (a) chaotic, so that the exponential separation of orbits generates the disorder needed in the model, and (b) with the same symmetries of the $q=3$ Potts model. A map that fulfills these requirements can be obtained as follows. Take the simple linear map, defined in the $[0,1)$ real interval

$$f(x) = \begin{cases} gx & \text{if } 0 \leqslant x < x_1, \\ a - gx & \text{if } x_1 \leqslant x < x_2, \\ b + gx & \text{if } x_2 \leqslant x < 1, \end{cases} \tag{2.2}$$

where g is the slope of the map, with $g>3$ so that the map is both chaotic and takes the $[0,1)$ interval *outside* of itself. The constants a, b, x_1, and x_2 are chosen so that $f(1/2)=1/2$, $\lim_{x\to 1} f(x)=1$ and the map is single valued and continuous. With these conditions, we get the following values for these parameters:

$$a = \frac{g+1}{2}, \quad b = 1-g, \quad x_1 = \frac{g+1}{4g}, \quad x_2 = \frac{3g-1}{4g}. \tag{2.3}$$

Now, put three of these maps together in the plane, joining the points $(1,1)$ of one map with the points $(0,0)$ of the next. This defines the segment $[0,3)$ as the domain. Finally, apply a modulo 3 operation to the outcome so that the range is also confined to the segment $[0,3)$. All together, the mapping becomes (see Fig. 1)

$$F(x) = [\text{int}(x) + f(x \bmod 1)] \bmod 3, \tag{2.4}$$

with f given in Eq. (2.2).

The model is completed by implementing a diffusive coupling scheme in a two-dimensional lattice of these maps. The definition for $\mathcal{D}$ in Eq. (2.1) is given as follows. Plot x and y along a circumference of perimeter 3 and take the shortest distance between them:

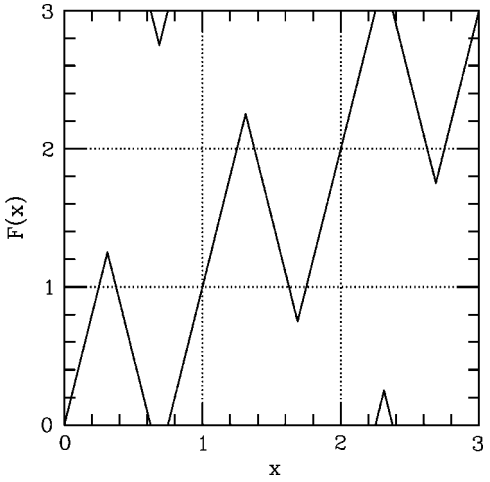

FIG. 1. Chaotic map for the dynamical analogous of the Potts model. The map is given by Eq. (2.4); the plot corresponds to the function $F(x)$ for $g=4$.

$$\mathcal{D}(x,y) = \begin{cases} x-y & \text{if } |x-y| < 3/2, \\ x-y-3 & \text{if } x-y > 3/2, \\ x-y+3 & \text{if } x-y < -3/2. \end{cases} \tag{2.5}$$

The complete dynamics is then

$$x_{i,j}(t+1) = \left\{ F(x_{i,j}(t)) + \frac{\epsilon}{4}\sum_{i',j'} \mathcal{D}(F(x_{i',j'}(t)),F(x_{i,j}(t))) \right\} \bmod 3. \tag{2.6}$$

The quantities to be studied are based on the local spins, defined as the integer part of x and taking, therefore, the values 0, 1, and 2. Upon this definition, it is easy to check that this model has the symmetries of the $q=3$ Potts model. In fact, the observables of this system are invariant when one applies the transformation $x \to x+1$, to the mapping (2.4), since one can show easily that $F((x+1) \bmod 3)=(F(x)+1) \bmod 3$. This generates the even permutations of the three states. Furthermore, the reflection of the variable around $x=3/2$ results in the reflection of F around the same value, and this generates the odd permutations.

From the spins we have defined we construct an instantaneous order parameter, defined as follows [21]. For a lattice of lateral size L let $n_q(t)$ be the number of sites whose state is q at time t, and let $n(t)$ be the greatest among them, i.e., $n(t)=\max[n_1(t),n_2(t),n_3(t)]$; then the instantaneous order parameter m_L^t is given by

$$m_L^t = \frac{3n(t) - L^2}{2L^2}. \tag{2.7}$$

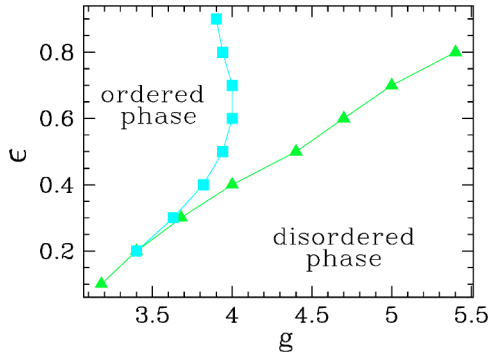

FIG. 2. (Color online) Phase diagrams corresponding to the synchronous (squares) and asynchronous (triangles) schemes; g is the slope of the chaotic map and ϵ is the coupling strength. The lines are given only as a guide to the eye.

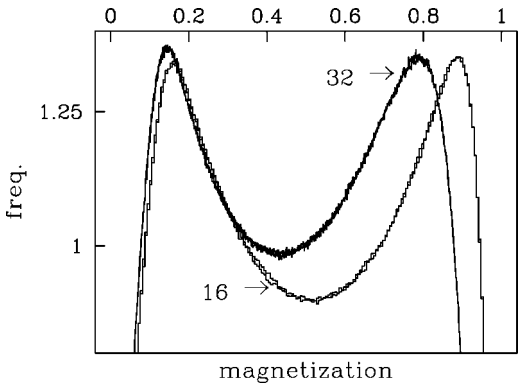

FIG. 3. Histograms of unit area for magnetization frequencies. There is one bin for each possible magnetization value. For each L there are two lines, one showing the histogram obtained from completely ordered initial conditions, and the other showing a histogram obtained from fully random initial conditions. The error bars (not shown) are of the order of the difference between the two lines. Here we use synchronous updating, $\epsilon=0.8$, with $g=4.0025$ for $L=16$, and $g=3.9733$ for $L=32$.

The order parameter M_L or magnetization is the time average of m_L^t, i.e.,

$$M_L = \langle m_L^t \rangle = \frac{1}{T} \sum_{t=t_0+1}^{t_0+T} m_L^t, \tag{2.8}$$

where t_0 is a transient time and T is the time interval over which the average is taken. Higher order moments of the magnetization are given by $M_L^{(q)}=\langle (m_L^t)^q \rangle$. A susceptibility is defined by

$$\chi_L = L^2 (M_L^{(2)} - M_L^2), \tag{2.9}$$

and the fourth-order cumulant [22,23] is

$$U_L^{(4)} = 1 - \frac{M_L^{(4)}}{3(M_L^{(2)})^2}. \tag{2.10}$$

III. SYNCHRONOUS UPDATING

We say the evolution of the system is synchronous when all the sites (i,j) of the lattice are updated in a single time step, as Eq. (2.6) suggests, taking as inputs the values of all the sites at the previous time. Following this scheme, after initializing the lattice with random numbers in the range $[0,3)$ and allowing the system to evolve for a transient time long enough for it to relax, we have studied its statistical behavior. We have found an order-disorder phase transition (PT) that depends upon the coupling intensity ϵ and the slope g of the chaotic map, as can be seen in Fig. 2, where a phase diagram is presented. A reentrant behavior is observed within a range of values for g, where the system can go from a disordered phase to an ordered one and back to the disordered phase as the coupling intensity increases.

A. Characterization of the phase transition

The PTs along the order-disorder boundary have been identified as continuous, as no hysteresis has been observed, and from the observation of the evolution of the probability densities for the magnetization. These probability densities were evaluated for three points along the order-disorder boundary, at $\epsilon=0.8$ and 0.9, varying g, and at $g=3.3$, varying ϵ. In all cases we found distributions with two peaks for the corresponding variable in the critical region, and have also found that these peaks become less pronounced as L grows, as shown in Fig. 3 for the $\epsilon=0.8$. In this figure we have plotted histograms for different values of the lattice size L; the frequencies have been normalized in such a way that the area below the histogram curve is 1. These histograms were averaged in periods of time long enough to obtain the same result, within error bars, regardless of the initial magnetization of the system. Even though the reduction of the distance valley peaks in the histograms is slow as L grows, the trend is clear enough. Following the criteria established for equilibrium systems by Lee and Kosterlitz [24], we take this transition to be continuous. Results for the other two points are quite similar. We are therefore taking this PT as continuous over the $0<\epsilon<1$ range.

B. Finite-size scaling and finite-size corrections

In order to find whether or not the model belongs to the universality class of the Potts model, we need to estimate the critical exponents for the system. To do so, we resort to the well-known approach of finite-size scaling, as described, for instance, in Ref. [25], including an estimation of the leading finite-size corrections (FSCs). The techniques involved have been described in Ref. [11], as well as in other reported work [10,20].

Our raw data are the measurements of the first four moments of magnetization—with corresponding error bars—for a large number of values of ϵ for fixed g or vice versa, and for several values of L. The first task is to estimate the critical coupling, be it g_c for fixed ϵ or vice versa. In what follows we will assume fixed ϵ and variable g. For this estimation we use the standard crossing of fourth-order cumulants

method ($U_L^{(4)}$ crossings), reported by Binder [22].

Even if this system is not a bonafide equilibrium system, we make the heuristic assumption that equilibrium results apply. This means that we can follow the standard formulation of scaling for equilibrium systems, in which one writes a free energy density for a system of size L as

$$F(g,H,L) = L^{-d}\hat{F}((g-g_c)L^{1/\nu}, HL^{(\beta+\gamma)/\nu}), \tag{3.1}$$

where H is an external magnetic field, d is the dimension of the lattice, and $\hat{F}$ is universal. Here we are ignoring both a nonsingular background and corrections to scaling. The critical coupling g_c and the critical exponents ν, β, and γ take their infinite-size lattice values. From here one finds that, in the absence of an external field, the magnetization M, the susceptibility χ, and the cumulant $U^{(4)}$ behave in the critical region as

$$M_L(g) = L^{-\beta/\nu}\hat{M}(L^{1/\nu}(g-g_c)), \tag{3.2}$$

$$\chi_L(g) = L^{\gamma/\nu}\hat{\chi}(L^{1/\nu}(g-g_c)), \tag{3.3}$$

$$U_L^{(4)}(g) = \hat{U}^{(4)}(L^{1/\nu}(g-g_c)), \tag{3.4}$$

where $\hat{M}$, $\hat{\chi}$, and $\hat{U}^{(4)}$ are universal functions.

Using these scaling assumptions, the standard crossing-of-cumulants method may be implemented in order to get the critical point [23], since Eq. (3.4) says that, in principle, cumulant curves should cross at the critical point g_c. In practice, when the lattice sizes are small, correction terms—which increase with decreasing lattice size—become larger than the statistical dispersion of the data and prevent the cumulant curves from having a common intersection. We are faced, therefore, with the need of dealing with FSCs. For systems in equilibrium, these correction terms originate in the irrelevant operators present in the free energy density, operators that typically scale with negative exponents as the size of the system grows. It is expected that, for L not too small, the irrelevant operator whose associated exponent has the smallest absolute value will dominate these corrections, where we are assuming simple power-law corrections. We have used different approaches in the estimation of g_c [11,14,20,22,26], and we are reporting the weighted average. Once an estimation of g_c has been achieved, we proceed to estimate the critical exponents using the customary expressions [11,14,20]

$$\partial_g U_L^{(4)}(g_c) \simeq L^{1/\nu}(A_0 + A_1 L^{-\Omega}), \tag{3.5}$$

$$M_L(g_c) \simeq L^{\beta/\nu}(B_0 + B_1 L^{-\Omega}), \tag{3.6}$$

$$\chi_L(g_c) \simeq L^{\gamma/\nu}(C_0 + C_1 L^{-\Omega}); \tag{3.7}$$

being A_0, A_1, B_0, etc., nonuniversal real parameters and Ω a nonuniversal effective correction exponent, different for each critical exponent.

C. Critical exponents

We have studied in detail, for a fixed coupling intensity (ϵ=0.8), the continuous PT that the system presents when the slope of the chaotic map varies. We worked with nine lattice sizes: L=16, 20, 26, 32, 40, 50, 64, 80, and 102. Correlation times are taken as $\tau_L = L^z\tau_1$ for a square lattice of side L, and from numerical simulations we get the estimates $z \approx 2$ and $\tau_1 = 0.898$. Transient times were taken to be $T_{trans}(L) = 4\tau_L$, the iteration time for a sample was set as $T_{iter}(L) = 500\tau_L$; and for each reported point in L and ϵ, no less than 200 samples were collected. These large amounts of data are reflected in the size of the uncertainties we get for the estimated averaged quantities.

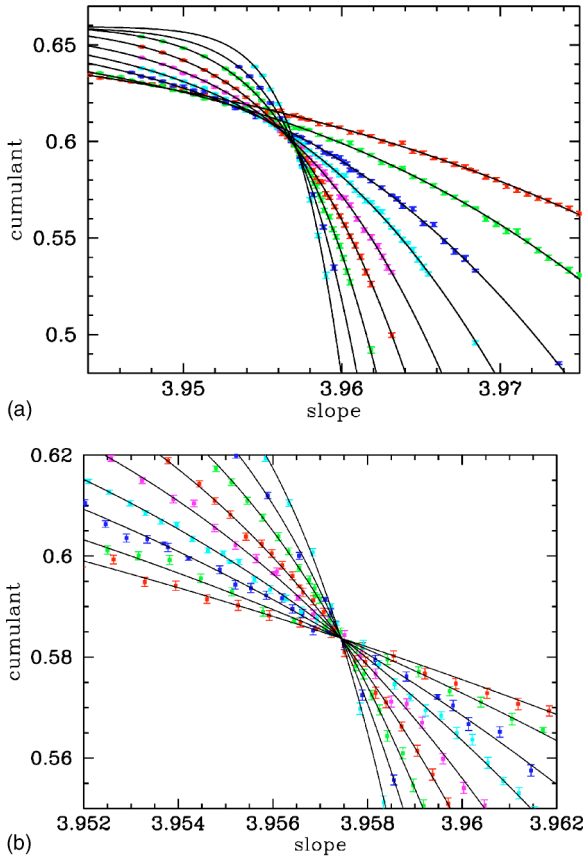

FIG. 4. (Color online) Estimation of the critical coupling for the model under the synchronous updating with fixed ϵ=0.8. (a) Fourth-order cumulant curves $U_L^{(4)}$ vs the slope g of the chaotic map. (b) Shifted cumulant curves, i.e., $U_L^{(4)}$ vs $g - AL^{-\Omega}$. The lines correspond to L=16, 20, 26, 32, 40, 50, 64, 80, and 102.

From the fourth-order cumulant we get a critical coupling g_c=3.9574(2) and a correction exponent Ω=2.4(2) (the numbers between the parentheses correspond to the uncertainty in the last digits of the quantity). In Fig. 4 we present, as an example, a plot of the original fourth-order cumulant curves $U_L^{(4)}$ vs g and the horizontally shifted curves $U_L^{(4)}$ vs $g - AL^{-\Omega}$, with a zoom around the critical point (crossings region). The values obtained for the critical exponents are ν=0.82(2), β/ν=0.15(1), and γ/ν=1.68(3). These values are to be compared with the reference critical exponents for the 2D Potts model (q=3), ν=5/6, β/ν=2/15, and γ/ν=26/15, which were obtained based upon a conjecture whose validity has been numerically verified (see Ref. [27]

and references therein). As can be seen, there is a good agreement between our estimate for ν and its exact value. Our β/ν and γ/ν show a marginal agreement with their exact values. We believe these deviations to be residual consequences of the strong FSCs present in the model. Therefore, we think the deviations found for these two exponents are not large enough as to constitute evidence to consider the model outside of the 2D $q=3$ Potts model universality class.

IV. ASYNCHRONOUS UPDATING

From among the many possible asynchronous updating schemes, we choose the most general one: For a lattice of side L, let $N=L^2$, then divide each time step into N substeps ($\Delta t=1/N$). In each of the substeps, update one element chosen at random so that in the long run each of the elements of the lattice gets updated once for each time step (a sweep of the lattice). Equation (2.6) becomes:

$$x_{i,j}(t+\Delta t)=\begin{cases}\left\{F[x_{i,j}(t)]+\dfrac{\epsilon}{4}\Sigma_{i',j'}\ \mathcal{D}[x_{i',j'}(t)-F(x_{i,j}(t))]\right\} & \text{mod } 3 \quad \text{if} \quad [i,j]=[\varsigma(t),\eta(t)] \\ x_{i,j}(t) & \text{if} \quad [i,j]\neq[\varsigma(t),\eta(t)],\end{cases} \tag{4.1}$$

where $\varsigma(t)$ and $\eta(t)$ are stochastic processes that take, at each substep, an integer value between 1 and L, with a uniform probability. As within the synchronous scheme, we have found an order-disorder phase transition that depends upon the coupling intensity ϵ and the slope of the chaotic map g, as can be seen again in Fig. 2, where the phase diagrams corresponding to both synchronous and asynchronous updating schemes are presented. A first difference between the dynamics of the system within different schemes is obvious; for the asynchronous scheme, the reentrant behavior is not observed.

A. Characterization of the phase transition

A very surprising result for the asynchronous updating of the model is that while for small coupling strengths the observed phase transition appears to be continuous, for large coupling intensities the system clearly presents a first-order PT. This is apparent from the absence of hysteresis in the first case and the development of strong hysteresis for the second, as shown in Fig. 5, where hysteresis curves for three different coupling strengths ($\epsilon=0.4$, 0.5, and 0.6) have been plotted. We have also studied the behavior of the magnetization histograms for ϵ close to ϵ_c. In Figs. 6(a) and 6(b) we present histograms of magnetization around the critical region, for two different coupling intensities: $\epsilon=0.2$, which is in the region where hysteresis is not observed, and $\epsilon=0.8$, in the region that presents hysteresis. As before, these histograms have been normalized in such a way that the area below the histogram curve is 1, and frequencies were averaged over times long enough to obtain the same result, within error bars, regardless of the initial magnetization of the system. For conditions under which the system does not present hysteresis [Figs. 3 and 6(a)], the trend is as expected for a continuous transition: two maxima are observed, but as L grows, the depth of the well between the peaks in the histogram decreases, and so, for large enough values of L, only a single peak is expected to appear. This signals that there is no coexistence of the ordered-disordered phases. On the other hand, the histograms corresponding to a large coupling intensity ($\epsilon=0.8$) within the asynchronous scheme, Fig. 6(b), show that the system can be either disordered or perfectly ordered, and the trend shows that as L increases, the separation between the perfectly ordered state and the disordered state is better defined, with a negligible probability for states in between; i.e., there is a clear coexistence of phases characteristic of first-order phase transitions. It should be mentioned that the ordered phase is not an adsorbing phase, since the lattice is entering and leaving this state as the simulation runs. It is clear therefore that there must be a tricritical

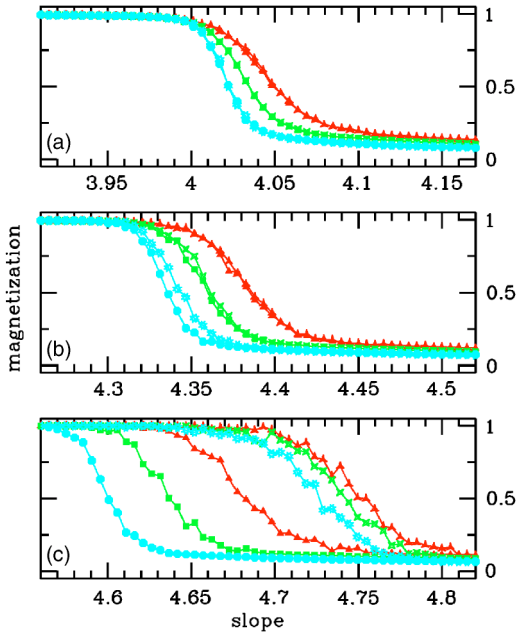

FIG. 5. (Color online) Hysteresis curves of magnetization for three different values of ϵ, and three different lattice sizes: $L=16$ (triangles), $L=20$ (squares), and $L=26$ (circles). Dark (light) points correspond to calculations in which initial conditions were fully random (completely ordered); in both cases, the transient time was taken to be of 10 000 time steps and the size of the interval for the average was of 50 000 time steps. Error bars are about the size of the marks.

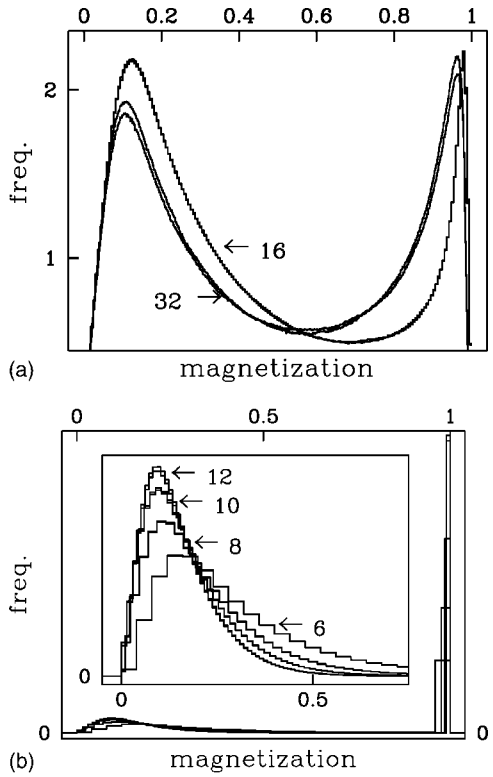

FIG. 6. Histograms of unit area for magnetization frequencies. There is one bin for each possible magnetization value. For each L there are two lines, one showing the histogram obtained from completely ordered initial conditions, and the other showing that obtained from fully random initial conditions. The error bars (not plotted) are of the order of the difference between the two lines. Here we use asynchronous updating, and the values of different parameters are (a) $\epsilon=0.2$, with $g=3.4197$ for $L=16$, and $g=3.4068$ for $L=32$; (b) $\epsilon=0.8$, with $g=5.6705$ for $L=6$, $g=5.5745$ for $L=8$, $g=5.5125$ for $L=10$, and $g=5.4685$ for $L=12$. Here, and in spite of the different heights, the extreme right bins have a total area of 0.5 in all the cases, meaning the system spends half of the time in a perfectly ordered state. The inset shows some detail of the histograms for the disordered phase.

point on the boundary between order and disorder in the phase diagram, but a precise numerical localization has not been achieved yet.

B. Critical exponents

For the region where the transition is second order, we have done numerical simulations in order to estimate the critical exponents for the system under this scheme. We have studied the continuous PT that the system presents when the slope of the chaotic map varies for a fixed coupling intensity ($\epsilon=0.2$). Here the correlation times for the dynamics are much larger than those for the synchronous updating; from numerical simulations we have estimated $z\approx 2$ and a τ_1 of 6.641. These large correlations make the simulations very time consuming, especially for large lattices, and so we have been forced to use only five lattice sizes: $L=16$, 20, 26, 32, and 40. We have used as before $T_{trans}(L)=4\tau_L$ and $T_{iter}(L)=500\tau_L$ for each sample, and obtained 100 or more samples for each L and ϵ simulated. We have followed again the crossing of fourth-order-cumulants method, and implemented finite-size scaling with finite-size corrections, as in the previous section. The value obtained for the critical slope was $g_c=3.4020(3)$, and for the correlation length exponent we found $\nu=0.72(6)$. This value of ν falls far away from the known value for the $q=3$ Potts model [27]. One needs to remember here that the presence of a tricritical point introduces a different universality class, and that for points that are not too far from the tricritical point there is always a crossover from the tricritical exponents to those of the continuous transition. At the moment we cannot yet rule out the possibility that the numbers we got might be just the results of such a crossover.

V. CONCLUSION

We have constructed a nonequilibrium, deterministic, and chaotic analog to the $q=3$ Potts model and have studied the order-disorder phase transition of this two-dimensional lattice of a chaotic coupled map whose dynamics has the $q=3$ Potts symmetry. We have found that the updating scheme is indeed a relevant parameter in the dynamical behavior of the locally coupled extended systems, since it can change the *type* of transition from continuous to first order. But contrary to the findings for dynamic [9–11] and stochastic [20] analogs of the two-dimensional Ising model, the critical exponent is consistent with the $q=3$ Potts model universality class. One then is faced with a question of why the behavior for the Ising model's dynamical and stochastic analogs with synchronous updating falls in a different universality class from that of the equilibrium Ising model. It should be noted besides that in this same class one finds the results for a simultaneous updating of a Metropolis-like algorithm on the Ising model. There is some reason therefore to believe that the deviation of the dynamic and stochastic models from the equilibrium universality class is an anomaly and applies only to models with the Ising symmetries.

Much more remarkable is the fact that, when studied within an asynchronous updating scheme, the model shows tricriticality; first-order phase transitions occur for large coupling and slope in the local maps (large chaoticity) and continuous transitions are found for small coupling and $g\approx 3$. Estimating the exact position of the tricritical point is still under work. The critical exponents we have found for the continuous phase transitions are not consistent with the $q=3$ Potts model universality class, but our numbers have to be taken still as preliminary, since the dynamics is quite slow under this updating scheme, and more statistics needs to be collected for good estimates to appear. Besides, it is quite possible that our numbers are simply reflecting a crossover phenomenon from the exponents associated to the tricritical point to those of the continuous phase transition. We have not tried to measure the exponent for the tricritical point yet.

The clear conclusion from the simulations performed for this model and from previous work [10,11], is that, for dynamical analogs of well-known equilibrium models, the updating scheme does matter. Thus, an updating scheme may give full agreement with the universality class of the corre-

sponding equilibrium model, while another may just change subtly the critical exponents, or change completely the character of the transition. This dependence with respect to upgrading schemes—or in general, to implementation of the model—extends even to their mean-field limits. For the Miller-Huse model it was found that a definition of the mean-field limit as a breakdown of closest-neighbor correlations gives a regular continuous transition in the mean-field universality class [28]. But an implementation of the same mean-field limit using fully connected graphs gives a first-order transition [29]. It is therefore clear that for these dynamical systems, symmetries, and range of interactions are not enough to predict their critical behavior.

ACKNOWLEDGMENT

This work has been supported by CONACyT, Mexico, through Grant No. 40726-F.

[1] K. Kaneko, Prog. Theor. Phys. **72**, 480 (1984).
[2] K. Kaneko, Physica D **37**, 60 (1989).
[3] K. Kaneko, Physica D **41**, 137 (1990).
[4] G. Pérez, S. Sinha, and H. Cedeira, Physica D **63**, 341 (1993).
[5] H. Chaté and P. Manneville, Chaos **2**, 307 (1992).
[6] H. Chaté and P. Manneville, Europhys. Lett. **17**, 291 (1992).
[7] H. Chaté and P. Manneville, Prog. Theor. Phys. **87**, 1 (1992).
[8] *Theory and Applications of Coupled Map Lattices*, edited by K. Kaneko (Wiley, New York, 1993).
[9] J. Miller and D. Huse, Phys. Rev. E **48**, 2528 (1993).
[10] P. Marcq, H. Chaté, and P. Manneville, Phys. Rev. Lett. **77**, 4003 (1996).
[11] P. Marcq, H. Chaté, and P. Manneville, Phys. Rev. E **55**, 2606 (1997).
[12] G. Vichniac, Physica D **10**, 96 (1984).
[13] N. Metropolis *et al.*, J. Chem. Phys. **21**, 1087 (1953).
[14] M. E. J. Newman and G. T. Barkema, *Monte Carlo Methods in Statistical Physics* (Clarendon Press, Oxford, 1999).
[15] G. Perez, F. Sastre, and R. Medina, Physica D **168–169**, 318 (2002).
[16] E. N. M. Cirillo, F. R. Nardi, and A. D. Plosa, Phys. Rev. E **64**, 057103 (2001).
[17] K. Kaneko, Phys. Rev. Lett. **65**, 1391 (1990).
[18] G. Abramson and D. H. Zanette, Phys. Rev. E **58**, 4454 (1998).
[19] S. Sinha, Int. J. Bifurcation Chaos Appl. Sci. Eng. **12**, 663 (2002).
[20] F. Sastre and G. Pérez, Phys. Rev. E **64**, 016207 (2001).
[21] S. Chen, A. M. Ferrenberg, and D. P. Landau, Phys. Rev. E **52**, 1377 (1995).
[22] K. Binder, Z. Phys. B: Condens. Matter **43**, 119 (1981).
[23] D. D. P. Landau and K. Binder, *A Guide to Monte Carlo Simulations in Statistical Physics* (Cambridge University Press, Cambridge, 2000).
[24] J. Lee and J. M. Kosterlitz, Phys. Rev. Lett. **65**, 137 (1990); Phys. Rev. B **43**, 3265 (1991).
[25] *Finite-Size Scaling and Numerical Simulation of Statistical Systems*, edited by V. Privman (World Scientific, Singapore, 1990).
[26] A. M. Ferrenberg and D. P. Landau, Phys. Rev. B **44**, 5081 (1991).
[27] F. Y. Wu, Rev. Mod. Phys. **54**, 235 (1982).
[28] S. Lepri and W. Just, J. Phys. A **31**, 6175 (1998).
[29] F. Sastre and G. Perez, Int. J. Bifurcation Chaos Appl. Sci. Eng. **10**, 251 (2000).